Supplementary information for: Requirements for Reversible Extra-Capacity in Li-Rich Layered Oxides for Li-Ion Batteries

Y. Xie[1,†], M. Saubanère[1,2] and M.-L. Doublet[1,2]

[1] *Institut Charles Gerhardt, CNRS - Université Montpellier 2,*

Place Eugène Bataillon, 34095 Montpellier, France.

[2] *Réseau Français sur le Stockage Electrochimique de l'Energie - RS2E FR3459, Amiens,*

France [†] *Permanent adress: Key Laboratory of Functional Inorganic Material Chemistry,*

Ministry of Education - School of Chemistry and Materials Science,

Heilongjiang University - Harbin 150080, PR China.

Computational details

Spin-polarized calculations were performed using the VASP code[1,2] within the density functional theory (DFT) framework. Perdew-Burke-Ernzerhof (PBE) functional[3] with a generalized gradient approximation form (GGA-PBE) was adopted to treat the exchange correlation energy. Due to the strongly correlated d-electrons, the rotationally invariant Dudarev method (DFT+U)[4] was applied for each transition metal for which different $U_{\text{eff}} = U - J$ ($J = 1$ eV) values were tested. The range-separated hybrid functional[5] (HSE06) was also used for a sake of comparison with DFT+U. To obtain a good numerical sampling of the electron densities in Brillouin zone, the Monkhorst-Pack technique[6] was used. According to our tests, it was found that the total energy difference obtained by using a (4×2×4) and a (6×4×6) Monkhorst-Pack mesh is smaller than 0.2 meV per forumula unit. Moreover, with the application of the projector augmented wave (PAW) technique,[7] the plane-wave energy cutoff was determined to be 600 eV. For structural relaxations, all atomic coordinates and lattice parameters were fully relaxed using the conjugate-gradient algorithm. The optimization procedure was repeated until the force acting on each atom is less than 3.10^{-3} eV.Å^{-1}.

The validity of the layered-type model was checked with respect to the publicly available datasets of the Materials Project initiative (MP).[8,9] For a sake of comparison with the data available in the MP, all Li_2MO_3 phases considered in this study (M = $3d$, $4d$, $5d$) were re-computed using the same numerical parameters as those used in the MP. As shown in Table S1, all M-based oxides are stable in the layered-type structure, except for M_{NS} = V, Cr, Nb, Hf, Ta for which formation energies were found above the convex hull by few tens of meV/at. Although metastable, these phases were kept in the study for a sake of comparison with the other phases and because partial M chemical substitutions using M_{NS} elements could lead to stable layered-type structures. Note that the asterix stands for the layered Li_2MO_3 phases which are not referenced in the MP dataset and whose formation energy was found below the convex hull of the today's available Li-M-O phase diagrams. According to these results, 76% of the Li_2MO_3 phases presently studied are stable which validates our structural model.

Table S1: List of "Stable" and "Not Stable" (NS) layered Li_2MO_3 phases, in which Stable*

stands for phases which are not referenced in the today available phase diagrams of the MPI and found stable in the present work. The d^n electron number corresponds to the electronic configuration of the M^{4+} oxidation state in Li_2MO_3.

	d^0	d^1	d^2	d^3	d^4	d^5	d^6
	Ti,Zr,Hf	V,Nb,Ta	Cr,Mo,W	Mn,Tc,Re	Fe,Ru,Os	Co,Rh,Ir	Ni,Pd,Pt
$3d$	Stable	NS	NS	Stable	Stable	Stable*	Stable
$4d$	Stable*	NS	Stable*	Stable	Stable	Stable	Stable
$5d$	NS	NS	Stable*	Stable*	Stable*	Stable	Stable

The reaction enthalpy associated with the formation of δ oxygen vacancy in Li_xMO_3 ($\Delta_r H$) was computed as a function of the Li content x for the series of $3d$, $4d$ and $5d$ metals using different U_{eff} values to account for the strongly correlated d-electrons. Volume effects (PV term) are usually small in condensed matter and can be generally neglected for such reactions. The oxygen molecule was treated in a $20 \times 20 \times 20$ $\mathring{A}^3$ periodic box and the additional term proposed by Ceder et al.[10] to correct the well-known overestimation of the O_2 binding energy was added to the O_2 DFT energy. Because we are seeking for trends, it was not necessary to include temperature effects in the calculations. The entropy of the reaction ($T\Delta_r S$) being dominated by the entropy of the O_2 gas, it is expected that the free energy of the reaction $\Delta_r G = \Delta_r H - T\Delta_r S$ would even favour O_2 release compared to $\Delta_r H$.
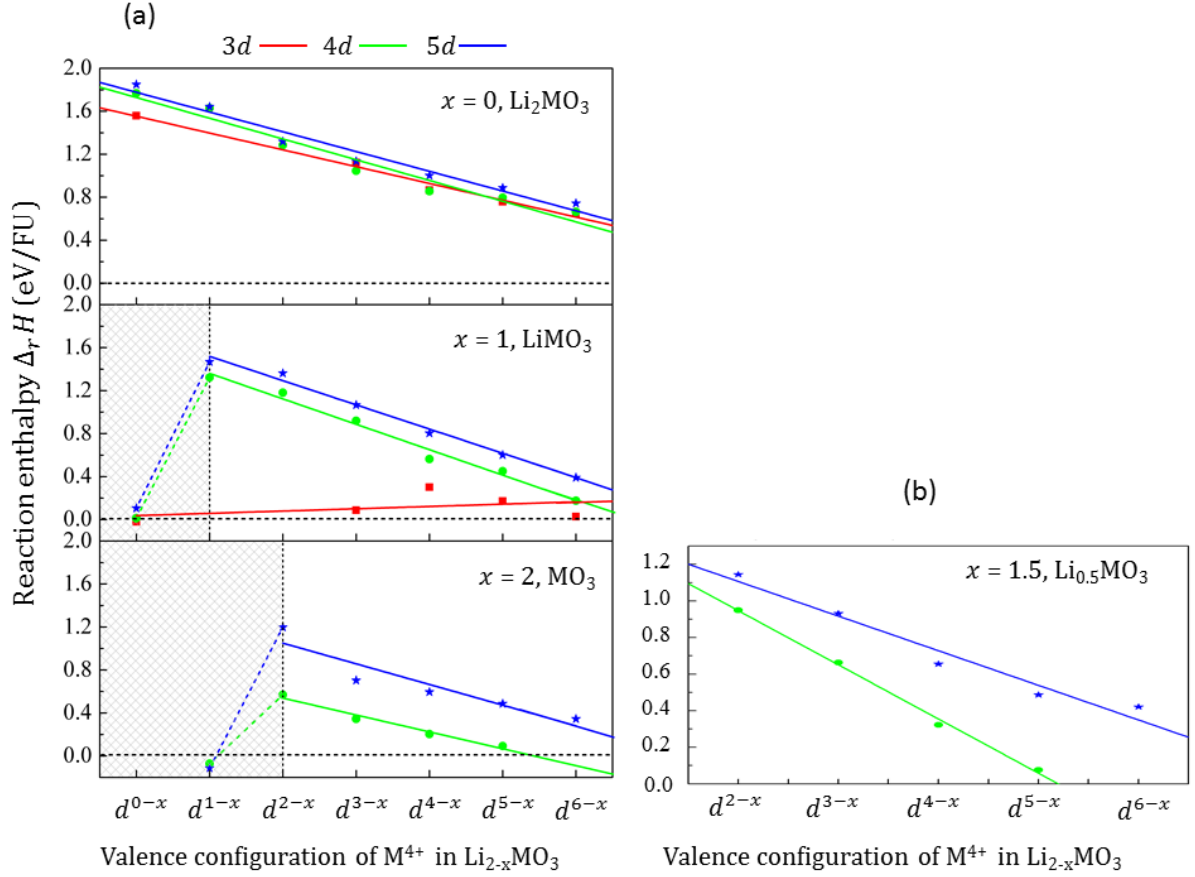
Figure S1: (a) Reaction enthalpies, $\Delta_r H$ in eV/FU, computed within the conventional DFT framework ($U_{\text{eff}} = 0$) and showing no significant variation from the one computed at $U_{\text{eff}} = 3$ eV (Fig.2 in the manuscript). (b) Reaction enthalpies computed for the intermediate lithium composition $Li_{0.5}MO_3$ and showing very similar results than for MO_3.
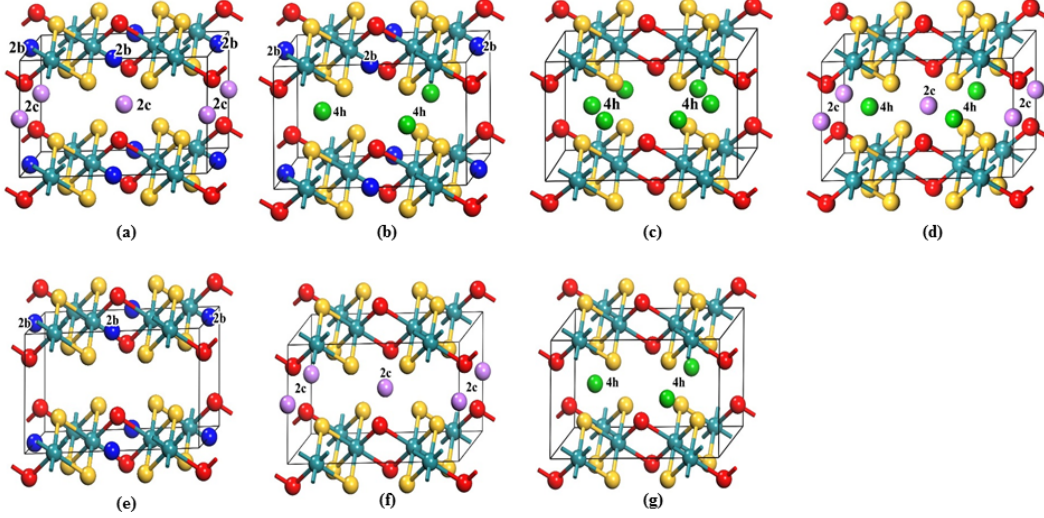
Figure S2: Different Li configurations considered in the calculations for the $LiMO_3$ phases (a-d) and the $Li_{0.5}MO_3$ phases (e-g). Our calculations show that when lithium occupies the $2b$ sites in the TM layer, the energy of the system is relatively higher than for the $2c$ and $4h$ sites. Previous theoretical calculations showed that the potentials required to remove Li from the TM and Li layers respectively are about 3.20-3.27 and 2.84-2.94 V in the $Li[Li_{(1-2x)/3}Mn_{(2-x)/3}O_2$ phase.[11] Experimental observations suggested that the depletion of Li^+ from the Li layer is compensated by the diffusion of Li^+ from the octahedral sites in the TM layer to the tetrahedral sites in Li-depleted layer.[12] Our calculations are then consistent with previous reports,[11–14] and the results discussed in the manuscript are based on the most stable structures obtained here.

Considering the oxygen vacancies, two independent positions labeled O_{4i} (red spheres) and O_{8j} (yellow spheres) were considered (see Fig.1 in the manuscript). In nearly all studied cases, our calculations suggest that the energies required to remove oxygen from one of these two positions are quite similar, but usually the ones for O_{8j} position are slightly smaller. Recently, Okamoto have examined the effect of oxygen vacancies in Li_2MnO_3 phase by first-principles calculations[15] and confirmed that O-vacancy in the $8j$ site is more stable than that in the $4i$ site by 0.10 eV per formula unit. Later, synchrotron XRD and Rietveld analysis on $Li_2MnO_{3-\delta}$ showed that the oxygen occupancy at $8j$ site decreases from 1.0 to 0.9646 after a low temperature reduction with metal hydride, while that at $4i$ site remains unchanged, leading to an oxygen deficiency of 0.071.[16] Only the configurations with the lowest energy were considered in the results presented in this work.

Table S2: Averaged change in the non-normalized oxygen-vacancy formation energy $\Delta_r H$ during Li-removal (eV/FU). The values for the Li_2MO_3 phases formed by $5d$ metals were taken as the reference energy.

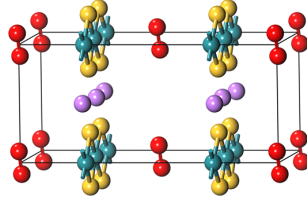|	$3d$	$4d$	$5d$
Li_2MO_3	-0.27	-0.05	0.00
$LiMO_3$	-0.98	-0.43	-0.18
MO_3	–	-0.92	-0.44

Figure S3: Crystal structure of the $LiNiO_3$ phase, as obtained after full structural relaxation and showing isolated O_2 molecules fully de-coordinated from the metallic network. Phonon calculation performed at the Γ-point of the Brillouin zone for this phase confirms its instability with six negative frequencies at -12.6, -22.71, -25.83, -28.13, -39.69, and -42.88 cm^{-1}.
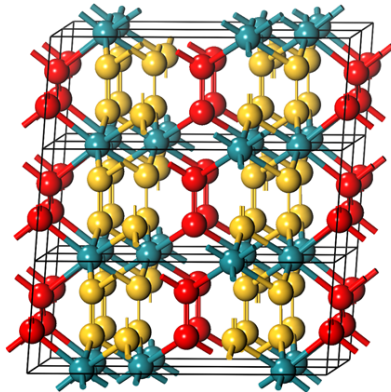
	$E_{\text{layered}} - E_{\text{condensed}}$
MnO_3	0.96 eV
FeO_3	1.00 eV
CoO_3	1.23 eV
NiO_3	1.18 eV

Figure S4 : Projection view of the condensed MO_3 phases obtained after full structural relaxation and showing the formation of short O-O dimers between the metallic layers to compensate the Li removal. In the table are reported the relative energies of the layered vs. condensed structures showing that the latter are much more stable than the former for the $3d$ series.
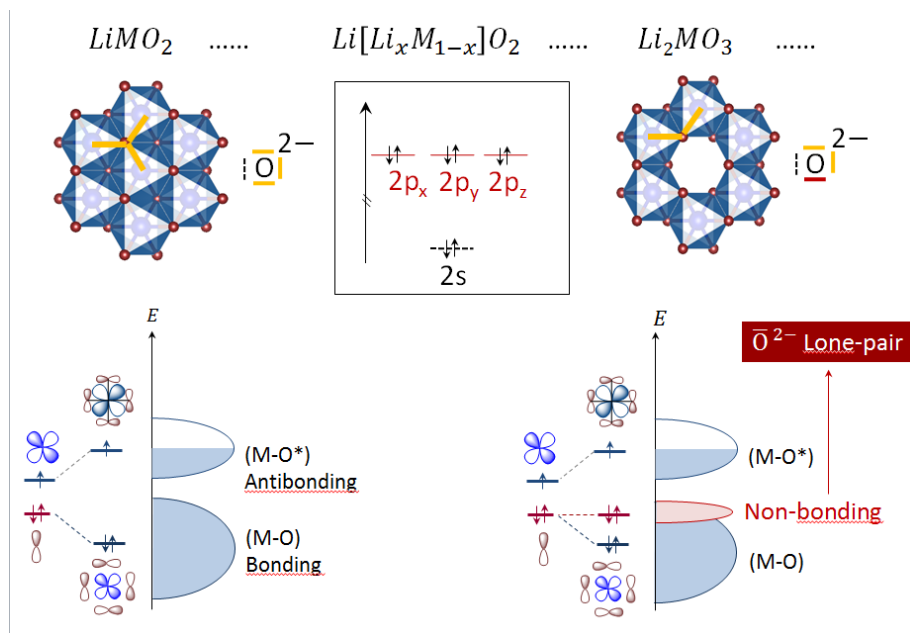

Figure S5: Illustration of the electronic band structure of $LiMO_2$ and Li_2MO_3 layered structures showing the occurrence of oxygen lone-pair states lying in between the bonding (M-O) and antibonding (M-O*) states when the O/M ratio is increased. The O^{2-} anion has four lone-pairs: one coming from the low-lying $2s$ orbitals and represented by the dashed black doublet and three coming from the high-lying $2p$ orbitals represented by the yellow doublets). Given the interactions in the metallic layer, each oxygen ion involves 2 ($LiMO_2$) or 3 (Li_2MO_3) of these doublets in the $M(d)$-$O(2p)$ interactions, leaving one non-bonded lone-pair in the Li_2MO_3 phase.
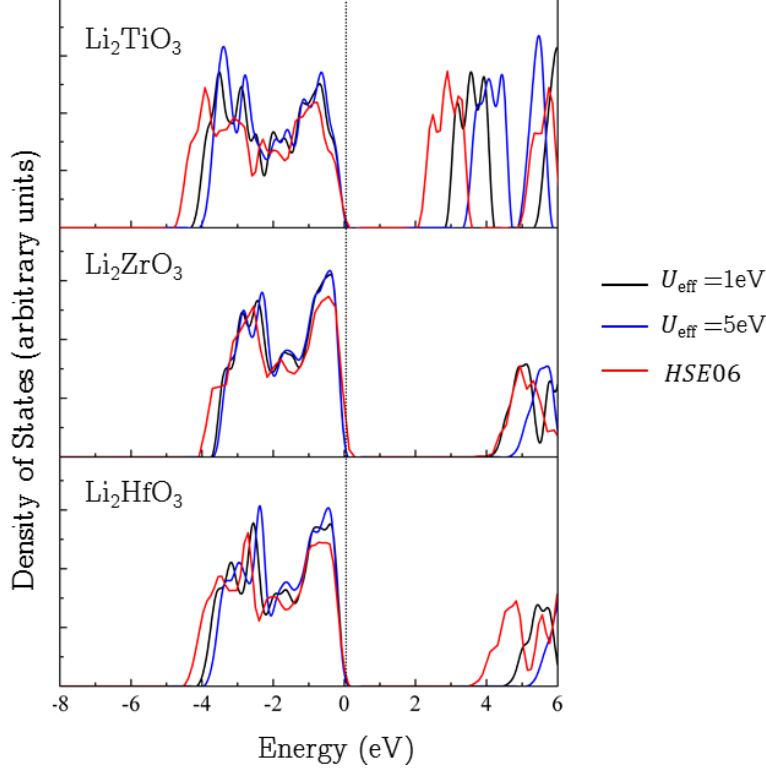
Figure S6: Density of states computed for the d^0 Li$_2$TiO$_3$, Li$_2$ZrO$_3$ and Li$_3$HfO$_3$ phases using different U_{eff} values of the DFT+U formalism and the range-separated HSEO6 functional. As expected for such charge-transfer insulators, the level of theory impacts on the band gap amplitude but not on the global shape of the electronic band structures.

Table S3: Shortest O-O distance observed in the fully relaxed Li$_{2-x}$MO$_3$ phases as a function of x and for all $3d$, $4d$ and $5d$ metals.

$3d$	$x = 0$	$x = 1$	x= 2	$4d$	$x = 0$	$x = 1$	x= 2	$5d$	$x = 0$	$x = 1$	x= 2
Li$_{2-x}$TiO$_3$	2.68	1.53	1.43	Li$_{2-x}$ZrO$_3$	2.83	1.54	1.46	Li$_{2-x}$HfO$_3$	2.82	1.54	1.46
Li$_{2-x}$VO$_3$	2.62	2.42	1.45	Li$_{2-x}$NbO$_3$	2.75	2.54	1.54	Li$_{2-x}$TaO$_3$	2.73	2.56	1.56
Li$_{2-x}$CrO$_3$	2.57	2.40	1.44	Li$_{2-x}$MoO$_3$	2.67	2.52	2.48	Li$_{2-x}$WO$_3$	2.67	2.52	2.45
Li$_{2-x}$MnO$_3$	2.57	2.45	1.40	Li$_{2-x}$TcO$_3$	2.75	2.45	2.40	Li$_{2-x}$ReO$_3$	2.79	2.47	2.41
Li$_{2-x}$FeO$_3$	2.59	2.41	1.39	Li$_{2-x}$RuO$_3$	2.72	2.57	2.37	Li$_{2-x}$OsO$_3$	2.74	2.60	2.40
Li$_{2-x}$CoO$_3$	2.48	2.37	1.37	Li$_{2-x}$RhO$_3$	2.69	2.55	1.43	Li$_{2-x}$IrO$_3$	2.71	2.50	2.37
Li$_{2-x}$NiO$_3$	2.50	2.44	1.37	Li$_{2-x}$PdO$_3$	2.72	2.60	1.35	Li$_{2-x}$PtO$_3$	2.74	2.58	2.51

1. G. Kresse and J. Furthmller, Efficiency of ab-initio total energy calculations for metals and semiconductors using a plane-wave basis set, Computational Materials Science, 1996, 6, 15-50.

2. G. Kresse and J. Hafner, Ab initio molecular dynamics for liquid metals, Physical Review B, 1993, 47, 558-561.

3. J. P. Perdew, K. Burke and M. Ernzerhof, Generalized Gradient Approximation Made Simple, Physical Review Letters, 1996, 77, 3865-3868.

4. S. L. Dudarev, G. A. Botton, S. Y. Savrasov, C. J. Humphreys and A. P. Sutton, Electron-energy-loss spectra and the structural stability of nickel oxide:An LSDA+U study, Physical Review B, 1998, 57, 1505-1509.

5. J. Heyd, G. E. Scuseria, M. Ernzerhof, Hybrid functionals based on a screened Coulomb potential, Journal of Chemical Physics, 2003, 118, 8207.

6. H. J. Monkhorst and J. D. Pack, Special points for Brillouin-zone integrations, Physical Review B, 1976, 13, 5188-5192.

7. P. E. Blchl, Projector augmented-wave method, Physical Review B, 1994, 50, 17953-17979.

8. S. P. Ong, L. Wang, B. Kang, G. Ceder Li-Fe-P-O2, *Phase Diagram from First Principles Calculations*, Chemistry of Materials, 2008 **20(5)**, 17981807.

9. A. Jain, G. Hautier, S. P. Ong, C. Moore, C. Fischer, K. Persson, G. Ceder, *Formation enthalpies by mixing GGA and GGA + U calculations*, Physical Review B, 2011, **84(4)**, 045115.

10. L. Wang, T. Maxisch and G. Ceder, Oxidation energies of transition metal oxides within the GGA+U framework, Physical Review B, 2006, 73, 195107.

11. C. P. Grey, W.-S. Yoon, J. Reed and G. Ceder, Electrochemical Activity of Li in the Transition-Metal Sites of O3 Li[$Li_{1-2x}/3Mn_{(2-x)}/3O_2$, Electrochemical and Solid-State Letters, 2004, 7, A290-A293.

12. M. M. Thackeray, S.-H. Kang, C. S. Johnson, J. T. Vaughey, R. Benedek and S. A. Hackney, Li_2MnO_3-stabilized $LiMO_2$ (M = Mn, Ni, Co) electrodes for lithium-ion batteries, Journal of Materials Chemistry, 2007, 17, 3112-3125.

13. Y. Shin, H. Ding and K. A. Persson, Revealing the Intrinsic Li Mobility in the Li_2MnO_3 Lithium-Excess Material, Chemistry of Materials, 2016, 28, 2081-2088.

14. Y. Koyama, I. Tanaka, M. Nagao and R. Kanno, First-principles study on lithium removal from

Li$_2$MnO$_3$, Journal of Power Sources, 2009, 189, 798-801.

[15] Y. Okamoto, Ambivalent Effect of Oxygen Vacancies on Li$_2$MnO$_3$: A First-Principles Study, Journal of The Electrochemical Society, 2012, 159, A152-A157.

[16] K. Kubota, T. Kaneko, M. Hirayama, M. Yonemura, Y. Imanari, K. Nakane and R. Kanno, Direct synthesis of oxygen-deficient Li2MnO3x for high capacity lithium battery electrodes, Journal of Power Sources, 2012, 216, 249-255.